TW2-TTMS-001b-D02

Task Title: IRRADIATION PERFORMANCE Neutron irradiation to 70 dpa at 325°C and PIE

INTRODUCTION

The main objective of this experiment is to study the irradiation behaviour of Reduced Activation Martensitic steels at high doses and for irradiation temperatures lower than 400°C, where materials are susceptible to reach a high level of hardening and embrittlement.

For this purpose, irradiations experiments are conducted in the BOR60 reactor of the Research Institute of Atomic Reactors (RIAR, Dimitrovgrad, Russia) at 325°C.

This task includes two items:

a) The Post Irradiation Examinations (PIE) corresponding to specimens irradiated in the first experiment (1st phase, ALTAIR experiment) in BOR60 that finished in 2002 for a dose of 42 dpa max.

b) A 2nd phase of irradiation (ARBOR 2 experiment) in the same reactor for 40 dpa at the same temperature that will allow to reach a dose of 70-80 dpa in specimens already irradiated in the 1st phase.

The European reference Eurofer 97 (9Cr-1WTaV) RAFM steel, experimental heats type 9Cr-2WTaV and ODS Fe-Cr alloys are included in both irradiations.

2004 ACTIVITIES

Specimens included in ALTAIR irradiation experiment have reached a dose ranging from 32 dpa up to 42 dpa. PIE started in 2003 and are conducted in hot cells of RIAR. In the first half of 2004, tensile tests and the measurements of reduction in area values of broken tensile specimens were completed. Also, the profilometry of pressurised tubes re-irradiated in ARBOR 2 experiment and that reached 63 dpa, was performed in June 04.

The installation of the impact machine in RIAR's hot cells was carried out in the first half of 2004. Charpy tests of ALTAIR specimens started in the last quarter 2004. Charpy data completion and other activities such as fractographic examinations and treatment of rough data to determine the energy transition curve for each material are planned in the first half of 2005.

Three progress meetings CEA - RIAR to exchange and discuss PIE progression were held in june, september and october 2004.

On the other hand, ARBOR 2 experiment, started in january 2003, goes on according to the initial schedule. The end of this irradiation is foreseen in the second quarter 2005.

MATERIALS / SPECIMENS

Materials irradiated in BOR60 are: Eurofer 97 (9Cr1WTaV), 9Cr2WTaV, 9Cr2WTaVB and ODS alloys. Chemical compositions and details of metallurgical conditions are given in [1].

RAFM steels, that is, Eurofer97, 9Cr-2WTaV and 9Cr-2WTaVB were produced as plates in the Normalized and Tempered (N&T) conditions.

ODS-MA957 ferritic alloy (Fe-14Cr-1Ti-0.3Mo) was produced as rod bars (8mm in diameter) with two different microstructures constituted by: a) Fine Grains (FG, 0.5 microns size) obtained after a stress-relieved treatment; b) recrystallised (R) grain structure (20-50 microns size) obtained with a recrystallisation treatment at 1100°C for 45 minutes.

Materials are irradiated as samples destined to mechanical tests. Three types of specimens are included:

1. Tensile specimens of 2 mm in diameter and 12 mm of gauge length obtained in the transverse direction in the case of RAFM plates, along the axial direction for ODS alloys.

2. Charpy subsize (KLST type) of 3 mm thick, 4mm wide and 27 mm long machined with TL orientation for RAFM steels, LT for ODS.

3. Pressurized tubes of Eurofer 97 and 9Cr2WTaV steels, for determination of in-pile creep. The dimensions of tubes are 6.55 mm and 5.65 mm respectively for the external and internal diameter and a total length of 55 mm. Tubes were machined in the transverse direction of plates. The junctions plug-tube were made by EB welding.

ALTAIR IRRADIATION EXPERIMENT (1ST PHASE)

This CEA irradiation experiment was shared with other material project. Specimens for the Fusion programme occupied 30% of the rig volume.

The rig of Altair was constituted of 7 levels or stages. The environment in the capsule was liquid sodium. The irradiation experiment was conducted over 12 irradiation cycles.

The maximum neutron flux was reached at the level 3 (see figure 1 of ref [1]) and the instantaneous maximum flux of fast neutrons (E > 0.1 MeV) corresponding to this level was about 2.00 ± 0.05 x 10^{15} n.cm^{-2} s^{-1}.

The average temperature of irradiation changes from different cycles, but the average values were always within the requested range 325°C ± 5°C for all levels.

Tensile and Charpy specimens of Eurofer 97, 9Cr-2W and 9Cr2WB were located in stage 3, those of MA957 FG and MA957R in the stage 2 and 7 and the pressurized tubes in the level 1 as indicated in table 1, where dose levels correspond to the experimental values measured by neutron detectors.

Table 1 : Materials and final doses attained by different types of specimens

Materials	Specimens	Level	Final dose
Eurofer 97 – 9Cr2WTaV	Pressurized tubes	1	41.9
ODS / MA957 (FG)	Tensile Charpy KLST	2	42.2
Eurofer 97 – 9Cr2WTaV - 9Cr2WTaVB	Tensile Charpy KLST	3	42.3
9Cr2WTaV – ODS / MA957 (R)	Tensile Charpy KLST	7	32.5

PROFILOMETRY OF PRESSURISED TUBES

The objective of profilometry measurements of pressurised tubes is to determine the deformation due to in-pile creep. The argon pressure inside the pressurized capsules was adjusted to induce a hoop stress level of 150 and 220 MPa at the irradiation temperature.

This type of measurements has been performed before irradiation, at the intermediary doses of 19.3 dpa, 41.9 dpa and after 63 dpa, the last value obtained in specimens re-irradiated in ARBOR 2 experiment. The weight of each pressurised specimen is also measured at each step to guarantee that there is not leakage of argon pressure. Figure 1 shows the average diametral strains determined for EUROFER 97 and 9Cr2WTaV RAFM steels compared to the 9Cr1Mo conventional martensitic steel. In all the cases, the strains measured are very low (< 1%) after about 63 dpa, confirming the rather good dimensional stability of ferritic-martensitic steels. To estimate the irradiation creep modulus, the following relation was used:

$$\varepsilon_\theta = 0.75\ A\ \phi t\ \sigma_\theta$$

where ε_θ is the diametral strain, ϕt the dose, σ_θ the average hoop stress and A the irradiation creep modulus. Contributions from swelling and thermal creep are assumed negligible.

Values estimated for the creep modulus are A = 0.4-1.0 x 10^{-6} $(dpa.Mpa)^{-1}$, which are in good agreement with values already determined for ferritic-martensitic steels at high temperatures (400-550°C).

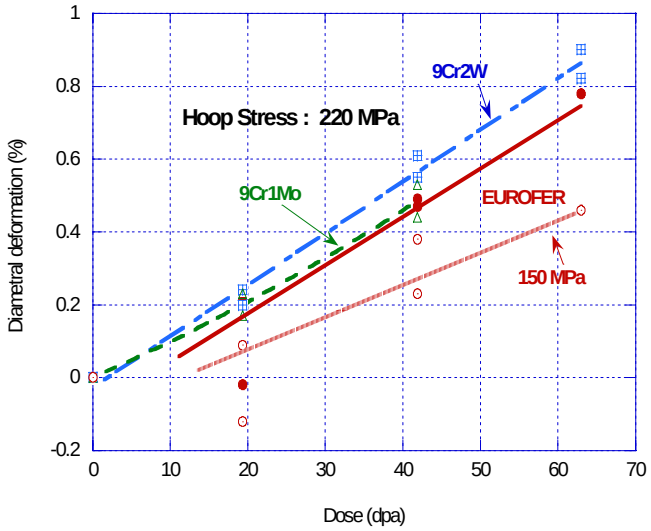

Figure 1 : Diametral strain of different materials as a function of the dose determined for a hoop stress of 220 MPa. In the case of Eurofer, an additional stress level, 150 MPa, is considered

TENSILE TESTS

Irradiated specimens were tested at 20°C and at the irradiation temperature (325°C) using a strain rate of 1.4x $10^{-3}s^{-1}$. Tests were also performed on control (unirradiated) samples for comparison.

The tensile properties of RAFM steels and ODS alloys are compared to those of commercial martensitic steels, standard 9Cr1Mo (EM10) and modified 9Cr1MoVNb (T91), irradiated in the same conditions.

Most of specimens considered in this report reached a dose in the range 40-42 dpa, except for 9Cr2WTaV RAFM steel and ODS-MA957 (R) in the recrystallised condition where the dose was 32.5 dpa.

Figure 2 shows the evolution of the tensile strength and the ductility after irradiation of different irradiated materials measured at the irradiation temperature.

As expected, all materials display an irradiation-induced hardening, determined by the increase of the yield stress, which depends on the material.

Hardening at 325°C is about 500-550 MPa for RAFM steels and ODS alloys, 600-760 MPa for conventional 9Cr1Mo steels. The ultimate tensile strength (U.T.S.) exhibits the same behaviour.

Specimens tested at room temperature exhibit an irradiation-induced hardening of about 10-15% higher than that determined at 325°C.

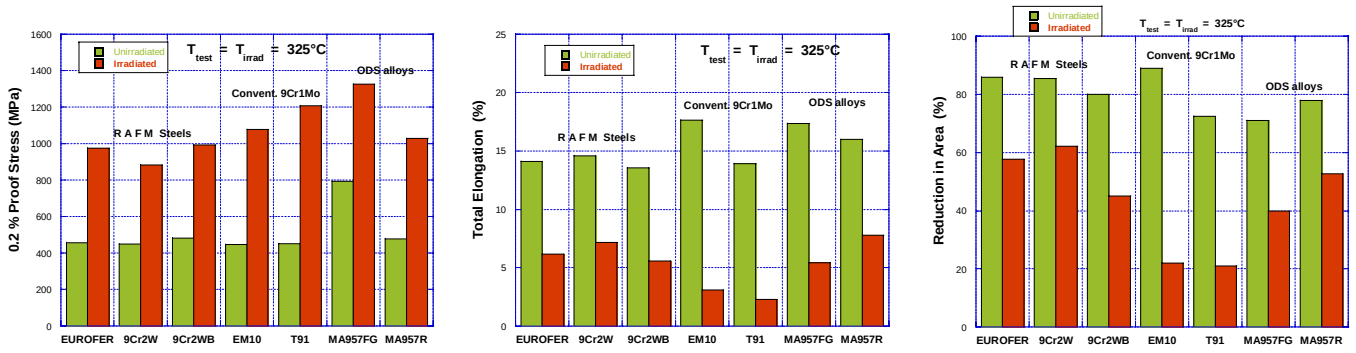

Figure 2 : Evolution of tensile properties of EUROFER 97, 9Cr2W RAFM, ODS alloys and 9Cr1Mo conventional steels after irradiation at 325°C for a dose up to 42.3 dpa. Measurements performed at the irradiation temperature

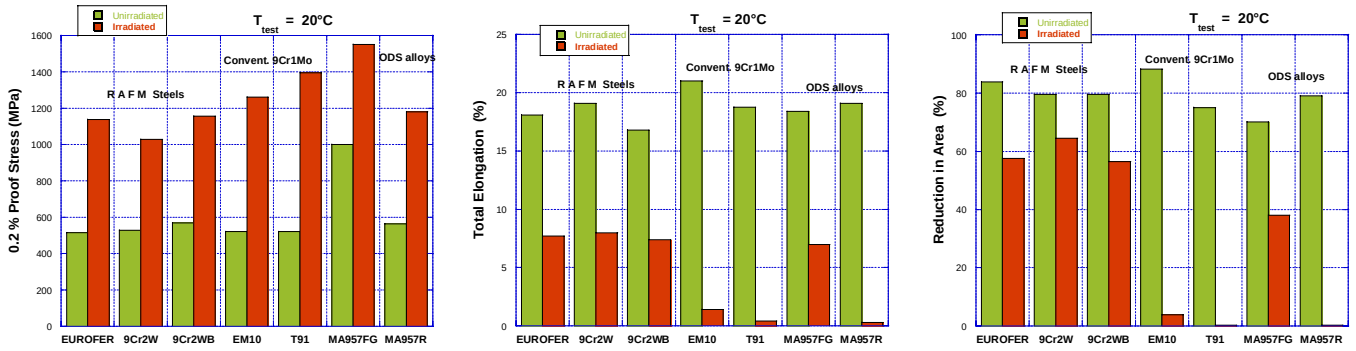

Figure 3 : Tensile properties of EUROFER 97, 9Cr2W RAFM, ODS alloys and 9Cr1Mo conventional steels after irradiation at 325°C for a dose up to 42.3 dpa. Measurements performed at room temperature.

The increase of tensile strength is associated to a reduction of the ductility, given by the decrease of total and uniform elongation as well as the reduction in area values, as shown in figure 2 for tests performed at the irradiation temperature. The loss of ductility at 325°C is more or less important depending of the material. A more dissimilar behaviour between materials was found for tests carried out at room temperature. In this case, some alloys like conventional 9Cr1Mo steels and ODS-MA957 recrystallised, evidenced a nearly total lost of ductility as illustrated by figure 3.

It is worthwhile to remark that the EUROFER 97 and RAFM steels present higher ductility and lower hardening compared to the conventional 9Cr1Mo martensitic steels irradiated in the same conditions. Also, ODS-MA957-FG fine grains, with an initial high tensile strength, presents after 42 dpa a relatively good level of ductility and the lower increase of tensile strength measured at both test temperatures.

CONCLUSIONS / FUTURE WORK

The irradiation behaviour of EUROFER 97, other RAFM steels and advanced ODS alloys are studied after irradiation in BOR-60 fast reactor at 325°C for high doses.

For this purpose, two experiments are performed: a) ALTAIR irradiation finished in October 2002 where the corresponding PIE are in progress, b) ARBOR 2 experiment that will end during 2005.

Materials reached in ALTAIR experiment a radiation damage ranging from 32.5 to 42.3 dpa. As expected, all materials harden during irradiation, but RAFM steels and in particular EUROFER 97, present the lower level of hardening and the higher ductility compared to conventional 9Cr1Mo steels. ODS-Fe-14%Cr-Y_2O_3 ferritic alloy, having a fine grain structure, display also an interesting behaviour as RAFM steels.

The profilometries of pressurised tubes of EUROFER 97 and other martensitic steels showed a very low irradiation-creep deformation at 325°C for doses up to 63 dpa.

Charpy tests to establish the energy transition curves are in progress and their completion is foreseen in the first half 2005.

A fraction of specimens irradiated in ALTAIR capsule are re-irradiated in the FZK/CEA common experiment ARBOR 2, also performed in BOR60 reactor. This one started on january 2003 and reached in october 2004 a dose of about 30dpa max, which means about 60-70 dpa in re-irradiated specimens.

REPORTS AND PUBLICATIONS

[1] A. ALAMO, J.L. BERTIN - Status of irradiation experiments performed in BOR 60 reactor at 325°C. Post-irradiation examinations of materials irradiated up to 42 dpa: 1st part - Progress Report TW2-TTMS-001b-D02 - CEA report DMN/SRMA/N.T. SRMA 2004-2679 - Dec. 2004.

TASK LEADER

A. ALAMO

DEN/DMN/SRMA
CEA-Saclay
F-91191 Gif-sur-Yvette Cedex

Tél. : 33 1 69 08 67 26
Fax : 33 1 69 08 71 67

E-mail : ana.alamo@cea.fr

Not available on line

Not available on line

Not available on line

Not available on line

Not available on line

Not available on line

Not available on line

Not available on line

Not available on line

Not available on line

Not available on line

Not available on line

Not available on line

Not available on line

Not available on line

Not available on line

TW4-TTMS-005-D01

Task Title: RULES FOR DESIGN, FABRICATION AND INSPECTION Update Data Base and Appendix A of DEMO-SDC

INTRODUCTION

Eurofer is a reduced activation ferritic / martensitic steel that has been selected as the European reference structural material for ITER Test Blanket Modules and DEMO reactor. Several industrial heats of this steel have been produced and tested within the framework of EFDA programme. The ultimate goal of these tasks is to propose materials properties allowables for design and licensing of components fabricated with the Eurofer steel.

TW4-TTMS-005 is one of the EFDA tasks that specifically targets structural materials rules, design and inspection. Its scope is extended since the year 2003 to include metallurgical and mechanical properties characterization actions that were previously carried out.

This report presents a summary of the work done during the year 2004 at CEA for the TW4-TTMS-005-D01. The work done is also part of an international collaboration, coordinated under the fusion materials implementing agreement of the International Energy Agency (IEA).

The main objective of the TW4-TTMS 005-D01 is to collect, validate and harmonize the results of Eurofer steel, in continuation of the earlier work done on the conventional 9Cr-1Mo steel and the RAFM steel grade produced in Japan (F82H), and propose materials properties allowables through an Eurofer steel specific Appendix A.

2004 ACTIVITIES

All actions and deliverables foreseen under the terms of TW4-TTMS-005-D01 have been fulfilled in time. In 2004, the database of Eurofer steel was updated, particularly with the RAFM data and analysis resulting from the work done at FZK / Germany.

With the addition of the new Eurofer steel data in 2004, the collection of relational databases for RAFM steels contains:

- Products database: 571 records including 118 on Eurofer.
- Compositions database: 475 records including 26 on Eurofer.
- Tensile database: 1018 records including 258 on Eurofer.
- Impact database: 1520 records including 467 on Eurofer.
- Impact plots: 161 records including 45 on Eurofer.
- Creep database: 205 records including 81 on Eurofer.
- Fatigue database: 181 records including 70 on Eurofer.
- Fracture toughness database: 78 records, including 48 records on Eurofer steel. 8 files are generated for a group of tests and 3 Master curves are plotted.
- Summary database of all above databases that allows sorting of all available test results for a given heat, product or sub-product.

Notice that each record contains many fields.

For instance, a single record of one tension test contains fields with inputs from specimen origin and geometry, its heat treatment and irradiation back ground, testing conditions and all the usual materials properties derived from such tests.

The updated database was then used to revise the Appendix A for Eurofer steel. Some missing design criteria were added. The full package sent to EFDA at the end of 2004 work contained:

- An updated Appendix A of the Eurofer steel referenced CEA-DMN/Dir TN 2004-02.
- A CD-Rom containing the Runtime Solution version 3.0 of the RAFM databases and related documents.
- A Getting Started note explaining how to use the Solution.

CONCLUSIONS

All deliverables foreseen in this action have been met. The revised Appendix A and its accompanying CD-Rom Runtime solution have been sent to EFDA and are now available to ITER and reactor design teams. In 2005 updating of the databases will continue, particularly with the post-irradiation test results, and data from ODS steels.

REPORTS AND PUBLICATIONS

F. Tavassoli - Fusion Demo Interim Structural Design Criteria (DISDC): Appendix A Material Design Limit Data - A3.S18E Eurofer Steel, EFDA Task TW4-TTMS-005-D01, CEA DMN/Dir TN 2004-02/A, Dec. 2004.

F. Tavassoli - Getting started with the RAFM Database Runtime Solution V. 3.0, EFDA Task TW4-TTMS-005-D01, CEA/Saclay, DMN/Dir, Oct. 14, 2004.

CD-Rom containing the Runtime Solution version 3.0 of the RAFM databases and related documents.

TASK LEADER

Farhad TAVASSOLI

DEN/DMN
CEA-Saclay
F-91191 Gif-sur-Yvette Cedex

Tél. : 33 1 69 08 60 21
Fax : 33 1 69 08 80 70

E-mail : tavassoli@cea.fr

TW4-TTMS-007-D02

Task Title: MODELISATION OF IRRADIATION EFFECTS Ab-initio defect energy calculations in the Fe-He system

INTRODUCTION

Ferritic steels are proposed as structural material in fusion reactors. When subject to 14 MeV neutron irradiation, large amounts of helium and hydrogen are produced from transmutation in addition to self-defects. High He concentrations in metals are known to induce microstructural changes such as bubble formation and void swelling. The objective of this subtask is to contribute to the modeling of such phenomena by providing a database at the *ab initio* level, i.e. in the framework of the Density Functional Theory (DFT), of energies and structures for a set of characteristic atomic configurations involving helium atoms and vacancies in the α-Fe lattice.

The present calculations are based on a fast DFT-code, namely SIESTA (Spanish Initiative for Electronic Simulations with Thousands of Atoms: http://www.uam.es/siesta) [1], [2].

This methodology was set up and validated last year by comparison with reference calculations based on plane-wave basis sets [6]. It has been applied here to predict the migration of interstitial and substitutional He atoms in α-Fe, and their interaction with other He atoms and with vacancies.

2004 ACTIVITIES

The results presented below are obtained at constant pressure, on 128 atom supercells, using 3x3x3 k-point grids for the Brillouin zone integration. All calculations are performed in the spin polarized Generalized Gradient Approximation (GGA).

HELIUM MIGRATION

Migration of interstitial helium

The migration of interstitial He is relevant to the initial stage after He implantation or He production by transmutation, before it is trapped by vacancies or other defects. According to the present calculations, interstitial He prefers to locate at tetrahedral sites rather than octahedral ones, the difference in solution energy being 0.18 eV. In the body-centred cubic structure, a tetrahedral solute may migrate between two equivalent sites without passing through an octahedral one (figure 1). We find for He a very low energy barrier, namely 0.06 eV, similar to the value of 0.08 eV found with an empirical potential [3]. It can therefore be concluded that the migration of interstitial He is extremely fast.

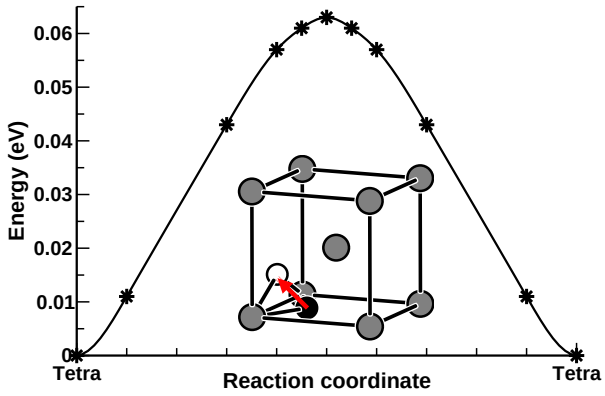

Figure 1 : Migration barrier of interstitial He in iron. The migration jump, between two tetrahedral sites, is schematically represented by the arrow between the initial site (in black) and the final site (in white) ; the iron atoms are represented in grey

Migration of substitutional helium

Two mechanisms are usually considered for the migration of substitutional He, either by vacancy or by dissociation [4]. The first mechanism requires another incoming vacancy. Let's first examine the energetics and local equilibrium geometries of configurations involving a substitutional He and a vacancy, i.e. two vacancies and a He atom. We find that the most stable configuration for the HeV_2 complex is when the two vacancies are first neighbors with a V to HeV binding energy of 0.78 eV, followed by the configuration where they are second neighbors, with a binding energy of 0.37 eV. The interaction between a substitutional He and a vacancy becomes negligible at third neighbor. Concerning the position of the helium atom, it is located midway between the two vacancies in the nearest neighbor case. For the second neighbor case, the helium atom also prefers to be off-site. In this case two degenerate positions exist, located at 0.25 times the lattice parameter from either of the two vacancies; they are separated by a barrier of 0.02 eV.

From the above configurations two competing two-step migration mechanisms can be inferred for the HeV_2 complex (figure 2 (a)-(e)). The first one involves a second neighbor intermediate configuration. First, a nearest neighbor jump of the vacancy transforms the nearest neighbor configuration into a second neighbor one; in the saddle point configuration He occupies a substitutional site (figure 2(d)). Then, by a similar but reverse jump, a nearest neighbor configuration is recovered. The corresponding migration energy is 1.17 eV. The second mechanism involves an intermediate configuration, the third neighbor one - where the He atom sits on one of the two vacancies - this configuration is higher in energy but actually has a slightly lower barrier (1.08 eV).

These barriers for are lower than the lower bound value of the vacancy dissociation energy from HeV_2 (1.45 eV), estimated from the sum of the V to He-V binding energy and the V migration energy (0.67 eV). Therefore the HeV_2 complex is expected to migrate as a unit over appreciable distances.

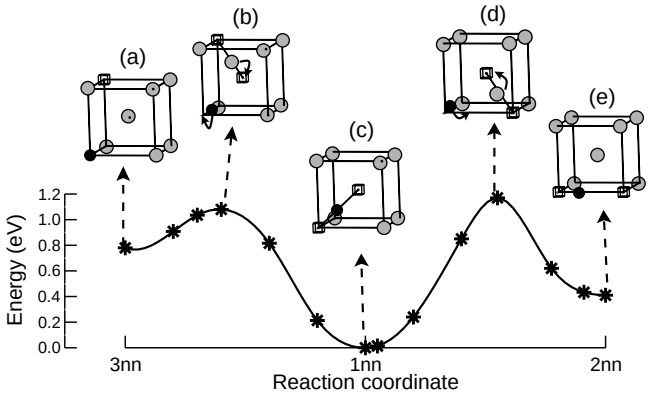

Figure 2 : Schematic representation of the energetic landscape and the most favorable migration mechanisms of the HeV_2 complex: (c), (e) and (a) represent the most favorable configurations when the He atom is bound to two first, second, and third neighbor vacancies respectively (b) and (d) are the saddle point configurations, the solid arrows indicate atomic jumps yielding configurations (a) and (e) starting from the ground state (c). The atoms (black spheres for He and gray spheres for Fe) are represented at their relaxed positions, vacancies are symbolized by small cubes

The effective migration energies of substitutional He can be discussed for the vacancy mechanisms described above and the dissociation one, i.e. when a substitutional He dissociates from its vacancy to migrate through interstitial sites until trapping at another vacancy. When thermal vacancies dominate, the expressions for these effective migration energies are [5]:

E^b (He-V) + E^m (He^{int}) – E^f (V)
migration by dissociation

E^m (HeV_2) + E^f (V) – E^b (He^{sub}-V)
migration by vacancies

where E^b (He-V), E^b (He^{sub}-V) are the tetrahedral He – vacancy, and substitutional He – vacancy binding energies respectively, E^f (V) is the vacancy formation energy, and E^m (He^{int}), E^m (HeV_2) are respectively the migration energies of a tetrahedral He and a HeV_2 complex.

The values obtained from the present calculations are 0.24 eV and 2.42 eV respectively.

When thermal vacancies prevail, the dominant diffusion mechanism is expected to be dissociative.

Note that empirical potential studies [3] give higher effective migration energies by dissociation, that is, 2.08 eV instead of 0.24 eV, mainly because of the larger predicted He-V binding energy.

BINDING OF HELIUM AND VACANCIES TO HELIUM-VACANCY CLUSTERS

Interaction between interstitial helium atoms

We find that the interaction between interstitial He atoms is attractive. The binding energy is 0.46 eV between the first two He atoms, and it increases with the number of He atoms. This self-trapping of He atoms together with the fast migration of interstitial He was proposed to be responsible for the formation of He bubbles observed at low temperatures in initially vacancy free lattices.

Interaction between substitutional helium atoms

We find that two substitutional He atoms prefer to be first nearest neighbors. The binding energy of two substitutional He located at first and second neighboring positions are respectively 1.15 eV and 0.74 eV, this attractive interaction is short ranged, the binding energy becomes negligible beyond second neighbor separation. When more than two substitutional He atoms are present, they tend to form compact clusters. We have investigated the binding energy of small clusters containing n He atoms (n = 2 to 5) according to the reaction:

$$He_{n-1}^{sub} + He^{sub} \rightarrow He_n^{sub}$$

The resulting values are 1.15 eV, 1.58 eV, 2.25 eV and 2.30 eV respectively, and the most compact clusters are the most favorable energetically.

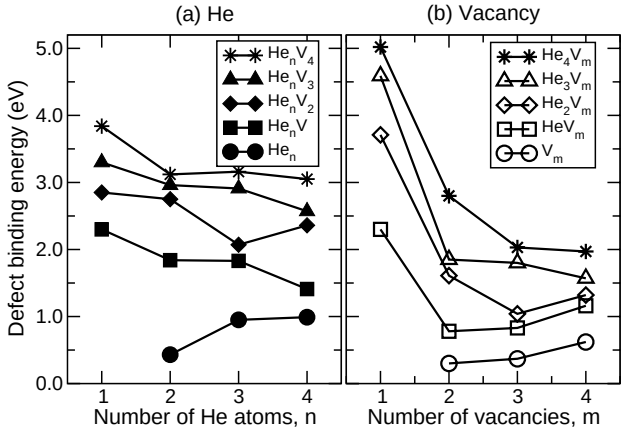

Figure 3 : Binding energies of (a) a He atom and (b) a vacancy to a $He_{n-1}V_m$ and He_nV_{m-1} cluster respectively. Abscises and legends refer to the composition of the resulting helium-vacancy cluster

Helium-vacancy clusters

More generally the stability of small He_nV_m clusters was also investigated for n and m = 0 to 4. The binding energy of a vacancy to the He_nV_{m-1} cluster is defined by:

$E_B(V)$ = E([N-(m-1)] Fe, n He) + E((N-1) Fe)
–E((N-m) Fe, n He) – E(N Fe)

where E((N-m) Fe, n He) is the energy of the system with (N-m) Fe atoms and a He_nV_m cluster.

The binding energy of an interstitial tetrahedral helium atom with a $He_{n-1}V_m$ can be defined in a similar way by:

$$E_B(He) = E((N-m)\ Fe, (n-1)\ He) + E(N\ Fe, He) - E((N-m)\ Fe, n\ He)$$

The convention adopted here is a positive sign for an attraction between the vacancy or the helium atom and the initial He-V cluster. They correspond respectively to the reactions:

$He_nV_{m-1} + V \rightarrow He_nV_m$ and
$He_{n-1}V_m + He^{int} \rightarrow He_nV_m$

where He^{int} indicates an interstitial tetrahedral helium atom. The values found are positive for all cases (figure 3). For n=1, the He binding energy increases as function of the number of vacancies in the cluster, m (see figure 3); it tends rapidly to the asymptotic value of interstitial He solution energy, i.e. 4.39 eV in the present calculation.

For a given value of m, the He binding energy decreases as the He content increases, reflecting the increase in cluster pressure caused by the accumulation of He atoms. Empirical potentials show the same trend, and predict a spontaneous emission of He or self-interstitials at larger n/m ratios [3].

The vacancy to cluster binding energies increase with helium content - again as a consequence of the increase of cluster pressure - and in particular they are always larger with than without helium (figure 3). In other words helium stabilizes vacancy-type clusters by reducing the vacancy emission rates.

This is consistent with the experimental evidence that He atoms enhance the formation of microvoids. For a given number of He atoms, n, the vacancy binding energy first decreases rapidly when the number of vacancies increases, until m-1 ≈ n, i.e. until the cluster pressure is reduced. Then, it increases slowly (as in the helium-free case), when the cluster surface energy contribution becomes dominant.

CONCLUSIONS

The following conclusions can be drawn from the present *ab initio* calculations on the behaviour of helium in pure α-Fe, and its interaction with vacancies:

- The migration energy of interstitial He, between two tetrahedral sites, is very low: 0.06 eV.

- The interaction between interstitial He atoms is attractive, with a binding energy of 0. 46 eV; this attraction is at the origin of the self-trapping effect proposed for He in metals.

- The interaction between substitutional He atoms is attractive, with a binding energy of 1.15 eV at nearest neighbor and 0.74 eV at second nearest neighbor.

- More generally the binding of He and vacancies to He_nV_m clusters have been determined up to n=4 and m=4.

- The migration barrier for the HeV_2 complex has been determined: 1.08 eV. It is involved in the migration mechanism of substitutional He by the vacancy mechanism.

REFERENCES

[1] J.M. Soler, E. Artacho, J.D. Gale, A. Garcia, J. Junquera, P.Ordejon and D. Sanchez-Portal - J. Phys. Cond. Matter 14, 2745 (2002).

[2] C.C. Fu, F. Willaime and P. Ordejon - Phy. Rev. Lett. 92, 195503 (2004).

[3] K. Morishita, R. Sugano, B.D. Wirth and T. Diaz de la Rubia - Nucl. Instr. Meth. B 202, 76 (2003) and references therein.

[4] L. K. Mansur, E. H. Lee, P. J. Maziasz and A. P. Rowcliffe - J. Nucl. Mater. 141-143, 633 (1986).

[5] V. Sciani and P. Jung - Rad. Eff. 78, 87 (1988).

REPORTS AND PUBLICATIONS

[6] F. Willaime and C. C. Fu - Ab initio calculations of helium-vacancy defects in α-Fe: first results - CEA report DMN/SRMP/2004-002/I.

[7] C. C. Fu and F. Willaime - Ab initio study of helium in α-Fe: dissolution, migration and clustering with vacancies - submitted for publication.

TASK LEADER

François WILLAIME

DEN/DMN/SRMP
CEA-Saclay
F-91191 Gif-sur-Yvette Cedex

Tél. : 33 1 69 08 43 49
Fax : 33 1 69 08 68 67

E-mail : fwillaime@cea.fr

TW3-TTMA-001-D04
TW3-TTMA-002-D04

Task Title: SiC/SiC CERAMIC COMPOSITES Divertor and Plasma Facing Materials

INTRODUCTION

The objective of these tasks is to irradiate in a common rig SiC-SiC ceramic composites and tungsten alloys samples at two temperatures, i.e., 1000°C and a lower temperature approximately of 600-650°C. The dose foreseen is about 5 dpa equivalent Fe. This irradiation experiment will be performed in the OSIRIS reactor at CEA-Saclay.

The first step of this work consists on the design of the corresponding irradiation capsule based on the requirements defined by EFDA for this irradiation experiment, i.e., conditions required, fluence level, temperature distribution, materials, type, number and dimensions of specimens.

As said before, two families of materials are planned to be irradiated in this experiment, that is, several types of SiC_f/SiC ceramic composites and refractory tungsten-based alloys. All materials will be supplied by EFDA as machined specimens ready for irradiation.

ACTIVITIES 2004

Activities performed during this period were mainly focused on the definition of the loading plan and the design of the irradiation rig. Also, the design of the gas circuit systems was continued as well as the safety analysis.

This experiment was named “FURIOSO” (FUsion RIg OSiris irradiatiOn).

LOADING PLAN

After several meeting and discussions, it was agreed the loading plan presented in table 1, which summarises the materials and the characteristics of specimens (type, dimensions and number) that will be irradiated in this experiment. Different nuances of SiC/SiC ceramic composites are considered for irradiation: 2D and 3D-composites supplied by EFDA and manufactured in Europe by MAN; 2D-NITE material from Japan and two types of composites supplied by ORNL (U.S.). These materials are included as specimens for mechanical tests (tensile and bending tests) and as samples for measurements of thermal diffusivity.

Concerning tungsten, two types of alloys will be included in the rig, one containing lanthanum oxide (W-La_2O_3) and other with potassium addition (W-K). These materials will be irradiated as plate tensile specimens and Charpy V subsize (KLST) samples destined to bending tests. The distribution and number of samples as well as the drawings giving the dimensions and the corresponding tolerances for each type of specimens have been communicated to EFDA for approval in october 2004.

IRRADIATION RIG

The irradiation capsule will be constituted of two sections of the same length, one that will work at 1000°C and the other at 600°C. Figure 1 shows a scheme of one irradiation temperature section of the sample holder. Each section is constituted of six baskets to locate the samples. SiC/SiC composite specimens occupy four baskets and W- samples are distributed in the two others.

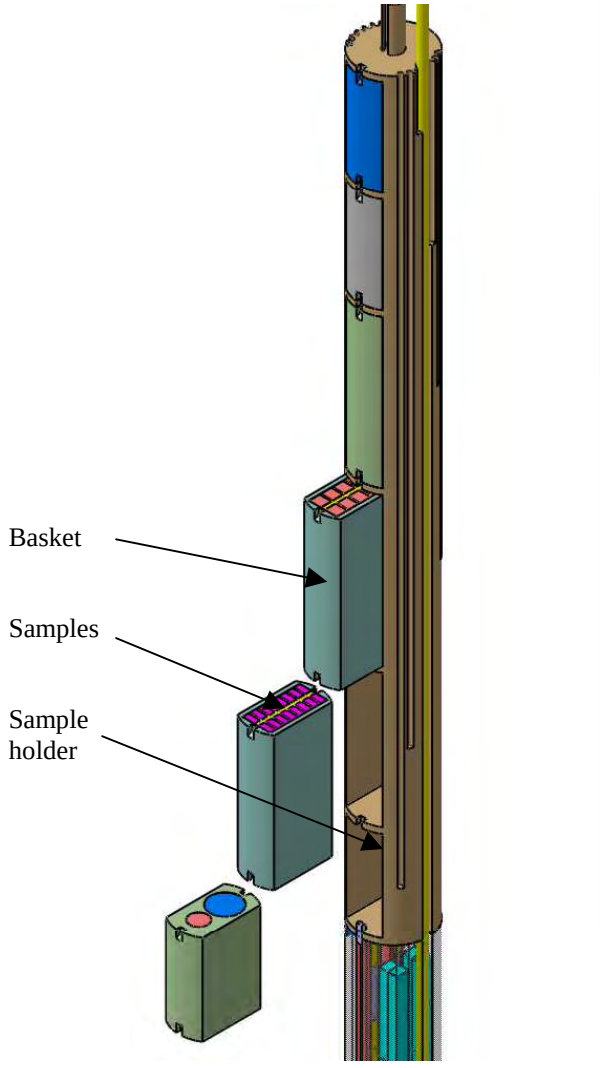

Figure 1 : Scheme of one irradiation temperature section constituted by six baskets for the distribution of different types of specimens

Table 1 : Loading plan : distribution of different materials and specimens in the rig

			Composites SiC / SiC				W- alloys	
	Temp. (°C)	Basket #	EU-3D	EU-2D	J-NITE	US	W1	W2
TOP	600°C	1					5Ch+3T19	
		2						5Ch+3T19
		3	4Bend+ 5T45	5T45				
		4	4Bend	6Bend				
		5			8T40	8T40		
		6	5D10	5D10	5D6	5D6		
	Isolating region							
	1000°C	7	5D10	5D10	5D6	5D6		
		8			8T40	8T40		
		9	4Bend	6Bend				
		10	4Bend+ 5T45	5T45				
		11					6Ch+3T19	
BOTTOM		12						6Ch+3T19
			Total number of specimens					
T40 : Tensile 4x2x40					16	16		
T45 : Tensile 4x2x45			10	10				
Bend : 4x3.5x45			16	12				
D6 : Diffusivity 0 6x2.5 thick					10	10		
D10 : Diffusivity 0 10x2.5 thick			10	10				
Ch : Charpy KLST							11	11
T19 : Tensile 5x1x19							6	6

(dimensions in mm)

The main concern in the design was related to the temperature distribution in the device because the materials behaviour is strongly dependent on the irradiation temperature. This parameter depends on the rig's position in the reactor core (gamma heating) and the geometry of the irradiation capsule.

The calculation and drawing of a powerful furnace were performed to guarantee the regulation and control of specimen's temperature during irradiation. But besides the heating system, the temperature could be also regulated, using a gas flow with an adequate thermal conductivity, inside and outside the sample holder. According to calculations of thermal distribution, a better control and regulation of temperature could be achieved using a flowing mixture of helium-neon for both internal and external gas circuits.

Consequently, inside the capsule, samples will be in contact with a circulating gas mixture of helium and neon. The final configuration of the gas control system is in progress. The monitoring of temperature will be performed with thermocouples located in the sample holder.

FUTURE WORK

At the present time, the design of the rig is practically finished as regards of the geometry and dimensions of the sample holder. Next time, the manufacturing of the sample holder will be launched. The completion of the design and the installation of the gas system are expected to be carried out in the first half of 2005.

TASK LEADER

A. ALAMO

DEN/DMN/SRMA
CEA-Saclay
F-91191 Gif-sur-Yvette Cedex

Tél. : 33 1 69 08 67 26
Fax : 33 1 69 08 71 67

E-mail : ana.alamo@cea.fr

TW4-TTMA-001-D04

Task Title: MODELLING OF THE MECHANICAL BEHAVIOUR OF ADVANCED 3D SiC_f/SiC COMPOSITE

INTRODUCTION

A previous bibliographic study indicate that modelling of the thermo-mechanical behaviour of SiC_f/SiC structure with multi-scale methods allows to introduce more physics by describing the phenomena that control its behaviour (damage, creep,…) at the scale at which they takes place [5].

The aim of the work performed in 2004 was to identify and gather the scale change methods, constitutive laws and representative volume elements the most adapted to SiC_f/SiC woven composites in order to perform their implementation in the finite element code CAST3M. This works results of a collaboration with the ONERA (Office National d'Etudes et de Recherches Aérospatiale) and the LCPC (Laboratoire Central des Ponts et Chaussés).

2004 ACTIVITIES

Two sets of constitutive laws (linking the stress to the strains) were chosen in order to allow comparison and mutual enrichment of the models.

Figure 1 shows on the left-hand the detailed structure of SiC_f/SiC woven composites.

Two successive scale changes at least are necessary. One from the macro (structure) to the meso scale (plies) and one from the meso to the micro scale (fibre, matrix and interface).

The right-hand of figure 1 shows the two sets of chosen representative volume elements at the different scales and indicate the change scale methods we will adopt.

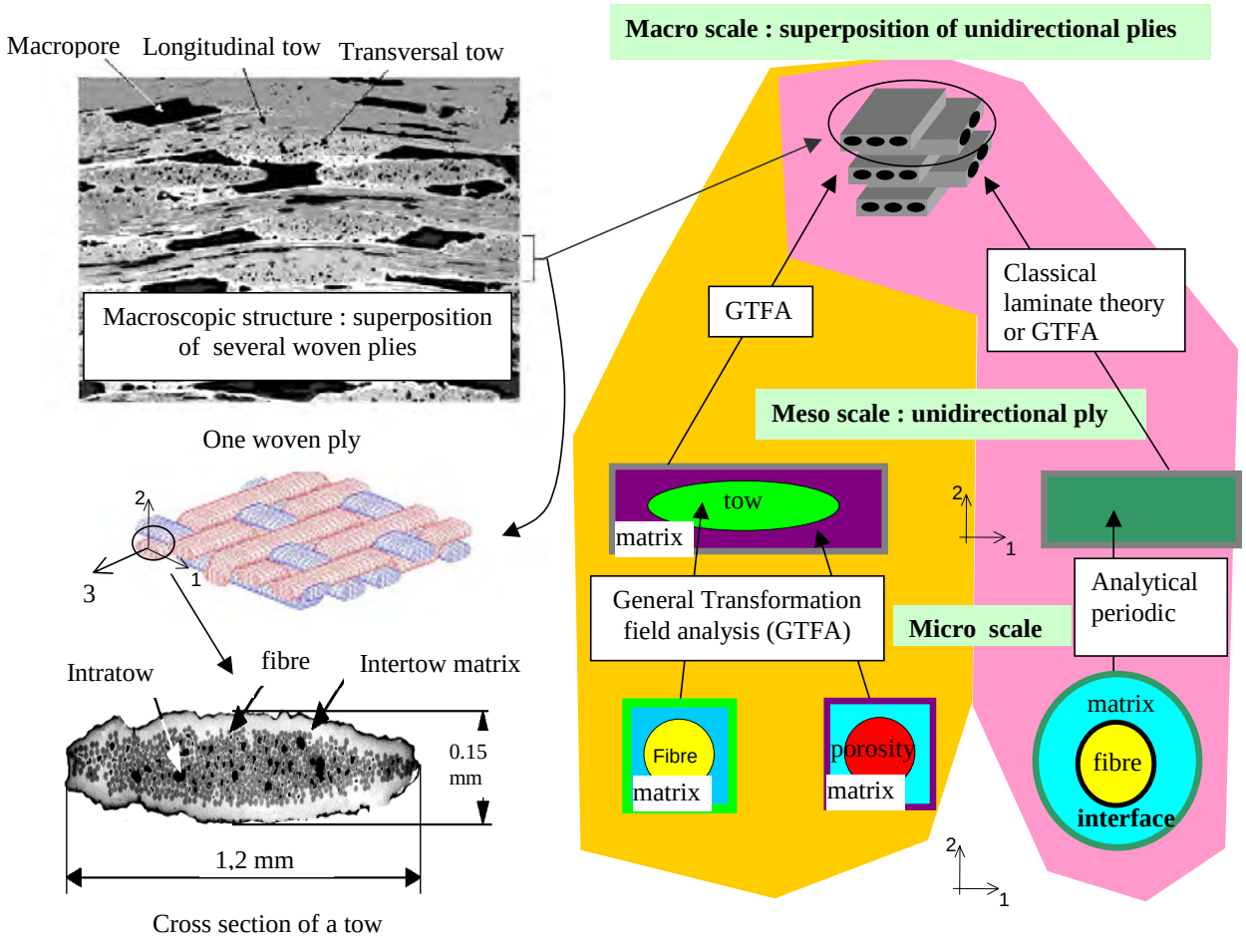

Figure 1 : Left-hand : detailed representation of woven SiC_f/SiC composite(from [4] [6] and [7]) Right-hand, representative volume elements and change scale methods chosen for the implementation in CAST3M (Yellow: from [6] [7], Pink: from [1] [2])

The first chosen constitutive laws set was reported by C. Rospars et al [1] [2]. These laws take into account the effect of damage at the level of the fibres, interface and matrix.

Their parameters have already been determined by C. Rospars for different SiC_f/SiC and C/SiC composites. These constitutive laws were moreover successfully applied to modelling of SiC_f/SiC structures via two scale changes. The other constitutive laws we wish to use were determined by ONERA [6].

They allow to take into account various phenomena observed during ceramic matrix composite testing such as the initial and damage-induced anisotropy (with the eventual lost of orthotropy), damage kinetics for the different cracking modes (different crack families defined by their orientations), damage deactivation, progressive cracks closure and residual strains induced by damage and residual fabrication stresses. These constitutive laws and their parameters are adapted and known for the macroscopic scale.

At lower scale, their parameters could be identified by inverse methods. It can also be envisaged to determine first the thermo-mechanical properties of the tows and the matrix with porosity using a multi-scale approach.

This allows to predict the influence of parameters such as fibres swelling or porosity concentration. Damage is then introduced at the meso-scale corresponding to the ply (sequenced method).

The change scale methods for the localisation step (calculation of the local strains, and corresponding stress, from the global strains) that will be used are the general transformation field analysis (GTFA) [7] and an analytical method for periodic fibre composites from C. Pideri [3] which is adapted to the micro to meso scale change. GTFA allows to perform all the envisaged scale changes. Constitutive laws as well as the change scale methods and the integrations methods are described in [8].

A UMAT procedure (procedure integrating the constitutive law that can be used in CAST3M or ABAQUS finite element code), based on the work of C. Rospars, has already been adapted to CAST3M and allows to calculate a unidirectional plane of SiC_f/SiC, corresponding to the meso scale.

The work which will be undertaken in the next years consists in the following points:

- Implementation of the GTFA method in CAST3M, including the calculation of the localisation and influence tensors for change scale (meso $\leftrightarrow$ macro) and (micro $\leftrightarrow$ meso).

- Implementation of the constitutive laws of ONERA for the scalar and pseudo-tensorial models.

- Tests calculations for the ONERA constitutive laws at the macro-scale.

- Following a sequenced integration method: determination of the thermo-elastic properties of the bundle and the matrix using multi-scale approach, introduction of damage at the meso-scale from the ONERA constitutive laws. Test calculations with scale change from meso to macro-scale

- The GTFA method for the meso to macro scale change (which allow to take into account out-of-plane 3D components) will also be used for test calculation of a realistic woven SiC_f/SiC composite with the micro to meso scale change and component constitutive laws of C. Rospars.

REFERENCES

[1] C. Rospars, E. Le Dantec and F. Lecuyer - CMC damage prediction by micro-macro modelling, twelfth international conference on composite materials - Paris, France, 5th-9th (july 1999) - ICCM-12.

[2] C. Rospars, E. Le Dantec and F. Lecuyer - Composites Science and Technology - 60 (2000) 1095-1102.

[3] C. Pideri - Matériaux composites élastiques - Thèse de l'université de Pierre et Marie Curie - Paris 6 - soutenue le 10 novembre 1987.

[4] V. Clard - Approches statistiques-probabilistes du comportement mécanique des composites à matrice céramique - Thesis n° 1948 - University of Bordeaux I - France, (1998).

REPORTS AND PUBLICATIONS

[5] C. Guerin - Multi-scale modelling for SiC_f/SiC composites - Preliminary considerations to an implementation in CAST3M - CEA report DRN/DMT SEMT/LM2S/RT/04-001/A - January 2004.

[6] J. F. Maire and N. Carrere - Modélisation multi-échelles des composites SiC_f/SiC - Définition des potentiels thermodynamiques et de dissipation pour les différents constituants du composites SiC_f/SiC (to be published).

[7] N. Carrere and J. F. Maire - Modélisation multi-échelles des composites SiC_f/SiC. Fourniture des éléments nécessaires à l'implémentation d'une méthode de changement d'échelle pour les passages micro-méso et méso-macro adaptée au SiC_f/SiC (to be published).

[8] C. Guerin - Multi-scale modelling of the thermo-mechanical behaviour of SiCf/SiC advanced composite - 2004 Activity report - Definition of the constitutive laws and gathering of the data necessary for the implementation in CAST3M (to be published).

TASK LEADER

Caroline GUERIN

DRN/DMT/SEMT/LM2S
CEA-Saclay
F-91191 Gif-sur-Yvette Cedex

Tél. : 33 1 69 08 53 52
Fax : 33 1 69 08 86 84

E-mail : cguerin@cea.fr

TW4-TTMI-001-D01

Task Title: IFMIF ACCELERATOR FACILITIES Accelerator system design

INTRODUCTION

The mission of IFMIF is to provide an accelerator-based, D-Li neutron source to produce high energy neutrons at sufficient intensity and irradiation volume to test samples of candidate materials up to about a full lifetime of anticipated use in fusion energy reactors. IFMIF would also provide calibration and validation of data from fission reactor and other accelerator-based irradiation tests. It would generate an engineering base of material-specific activation and radiological properties data, and support the analysis of materials for use in safety, maintenance, recycling, decommissioning, and waste disposal systems.

The basic approach is to provide two linacs modules, each delivering 125 mA at 40 MeV to a common target. This approach presents availability and operational flexibility advantages.

The Transition year(s) were initiated in 2003 with the objective of continuing the "Key Element Technology Phase" (KEP). The activities defined here concentrate on a follow up of the previous work, delivery to the other team of the previous works, transition meetings, reflection on the present design and it's possible evolution.

The IFMIF work is carried out at the CEA in the framework of a considerably larger activity presently undergoing in the field of high-intensity linear accelerators [1], [2], [3].

2004 ACTIVITIES

THE REFERENCE DESIGN

The ion source generates a Continuous Wave (CW) 140-mA deuteron beam at 95 keV. A Low Energy Beam Transport (LEBT) guides the deuteron beam from the operating source to a Radio Frequency Quadrupole (RFQ). The RFQ bunches the beam and accelerates 125 mA to 5 MeV. The 5 MeV RFQ beam is injected directly into a Room Temperature (RT), Drift-Tube-Linac (DTL) of the conventional Alvarez type with post couplers, where it is accelerated to 40 MeV.

The rf power system for the IFMIF accelerator is based on a diacrode amplifier operated at a power level of 1.0 MW and a frequency of 175 MHz. Operation of both the RFQ and the DTL at the same relatively low frequency is a conservative approach for delivering the high current deuteron beam with low beam loss in the accelerator. The use of only one rf frequency also provides some operational simplification.

Beam loss in the accelerator is to be limited so that maintenance can be "hands-on", i.e., not requiring remote manipulators. However, the accelerator facility will be designed in such a way that remote maintenance is not precluded. As shown later, the DTL output beam is carried to the target by a High Energy Beam-Transport (HEBT) that also provides the desired target spot distribution tailoring and energy dispersion. This HEBT must perform a variety of functions, complicated by the presence of strong space-charge forces within the beam.

The design improved since the referenced CDA in 1996. Several options were evaluated, and the work lead to the selection of a single reference for each subcomponent. There is no showstopper in the present reference design, but it does not mean that this 10 MW accelerator will be easy to build. Each subsystem will have to be carefully built and assembled. The project remains one of the most powerful in the word. The reference design is based on a conservative basis for this reason, most of the subcomponents having been fully tested or used. The design did not significantly change during the year 2004. The most interesting points are a confirmation on some choices.

Even if the reference design exists, the delays observed in the process of decision can be profitably used in exploring new possibilities, which will have to prove there ability to replace the present choices.

The ECR Source

The ECR source was selected as a result of the IFMIF KEP development program. This choice has been validated after extensive parallel development in Europe (CEA-Saclay and Frankfurt) and in Japan (JAERI). It has been selected mostly because of its intrinsic availability compared to other source types, and its efficiency. No further development on the D^+ source is required.

We need to use H_2^+ particles instead of D^+ during the commissioning of the accelerator in order to minimise the activation during the tuning. Therefore work was provided on this basis in CEA-Saclay and IAP-Frankfurt. In both places, the results are not in accordance with the objectives. The source is optimized for atomic ions production and extraction; it remains extremely difficult to tune it for molecular ions production. Around 30 mA can be extracted at the cost of a big amount of other species.

Opinion was received that H^+ could be used by running the accelerator at half voltage, thus avoiding the need for H_2^+ injector which requires development. The Accelerator Team does not fully agree with this position as it ignores the most important aspect of reliability. At half-voltage, the accelerator is not at its operating condition.

Extensive experience at LEDA showed that the most difficult conditioning and tuning problems occurred within 10% of the design conditions. The main (only ?) advantages of running H^+ is to check the obvious errors like quadrupoles misplugged or badly misaligned.

The requirement for an H_2^+ injector for commissioning and tuning will remain on the requirements list. This supposes the development of a new source, which has to start very soon in order to meet the requirement on time for the commissioning. As this new source will be used only during commissioning, it has to be easily plugged. Also one has to understand that the beam parameters (like emittance) will be different from the final source. A complete study will have to be made during EVEDA to assess the gain of such source. If no solution could be found, the commissioning will have to be made in pulsed mode to minimize the activation. The acceptable losses vs beam duty factor will have to be calculated by the safety group during EVEDA.

The whole accelerator has to be able to work also in pulsed mode, and this includes the source, the RF system and diagnostics.

Beam diagnostics

The development of diagnostics continues but is clearly not sufficient. The IFMIF program may profit from other project like SPIRAL2 [3], IPHI [1] or SNS [4], J-Park [5] and GSI [6] in order to develop non interceptive diagnostics. Some techniques are promising like the Doppler shifted line analyses or the backscattered particles detection that will be use during the IPHI tests in Saclay, or the profiler based on residual gas ionization in use in GANIL.

Nevertheless the specificity of the IFMIF accelerators (very high beam power, low energy) makes the development crucial. They are also difficulties in finding good diagnostics for the longitudinal plane (transition RFQ-DTL and DTL tanks). It appears that the beam footprint monitoring instrumentation is not needed any more. This is a good point that needs to be clarified, as it is a crucial point at the intersection of 2 groups : target and accelerator.

Beam diagnostics specific to IFMIF have to be developed during EVEDA.

RFQ

RFQ are expensive components. They are also crucial to bunch and accelerate the beam. The output beam energy has been part of an optimization of the whole design, and decreased from 8 to 5 MeV in 1999.

There are 2 designs available, with similar performances. They were compared with different codes. It is important to know that only one of the 2 (the Saclay design) was used in the end-to-end error study performed by the Saclay group, including the HEBT. Also the Saclay team has performed SUPERFISH calculations and 2D shape optimizations which provided good RF power consumption.

The tuning knowledge of 4-vanes RFQ was a result of a strong CEA effort. It might be exported.

Two types of cavity were evaluated for the IFMIF accelerator: 4-vanes and 4-rods types. One can quote that:

- Four vanes structures are the less consuming structures.
- Four rods RFQs show a very high peak power loss. The value cannot be easily managed and induces engineering difficulties and possible deformations in CW mode.

The Frankfurt team looked seriously in the 4-rod options and recommends, as us, using 4-vane RFQ.

Taking these results into account, we reinforce our recommendation using the 4-vane RFQ type.

The 2-D transverse section is completely defined. The optimization leads to an RF consumption estimated to ≈ 1600 kW, “everything” included. One RF source has been saved.

The work that needs to be done concerns the RF coupling in the cavity (engineering), the optimization of the 3D extremities, detailed design and integration. A high power RFQ cavity load must be build. It will help the design and will be useful as a load for the RF system and coupling loop tests. Tests using beam injection should also be included. Obviously, if the budget profile allows a fully-constructed RFQ, time and money will be saved.

DTL

A good and conservative design exists. It was included in the multiparticle end-to-end beam simulations performed in 2003. A hot model had good success in proving the feasibility. This hot model was developed at 352 MHz with similar or stricter parameters.

Detailed design and integration have to be performed. Engineering prototypes at the right frequency for manufacture of the DTL is now required. The RF coupling to the cavity has also to be studied.

The IFMIF High Energy Beam Transport line

The HEBT was studied based on the reference concept (multipole expanders). It reaches performances close to the requirements. Nevertheless the differences need to be validated by the target group.

The detailed design and integration of the line needs to be done. This will include the magnet specifications. The HEBT scrapers must be studied, and may have an impact on the line length (shielding).

We already know that the magnetic elements of the end part of the line will have to be aligned with concepts coming from the 4^{th} generation electron light machine. Their placement and displacement will have to be monitored with an active system (2 µm).

A cheaper solution may exist with a raster scanner technique. A safe and rigorous system may be built with a good benefit for the project.

RF system

We now have at least one manufacturer able to deliver a 1MW CW tube at 175MHz. The tube was tested for more than 1000 hours on a dummy load with success.

The RF system remains the most expensive part of the accelerator. Therefore it is necessary to have a good control of the costing of these elements. We recommend to quickly developed, buy and test a full RF system. An experienced team is already working on this topics, it is a good point to maintain.

The test can be made on the RFQ hot cavity, with beam coming in (test of the RF low level, RF high level, and beam injection capability). This supposes the availability of a test stand, as always stated by the accelerator group.

Miscellaneous

- The first point concerns the test stand. As stated by R. Jameson: "Probably the largest "hole" in the EVDA definition is that the costs for the engineering validation tests assume the existence and underwriting of a powerful test facility, capable of installing and operating the D^+ and H_2^+ injectors, RFQ load cavity, complete RF system with one coupler, and beam diagnostics instrumentation (…/…) as a test stand".

- The safety analysis should start as soon as possible. It has a big impact on the accelerator and building designs. Experience with other projects showed that it may also lead to huge planning delays if not started on time. A call for work package was tendered by EFDA.

- The main beam parameters are defined at low energy. So, if one wants to qualify the accelerator, it is necessary to build and test a source, LEBT, full RFQ and the first tank of the DTL. This will have to be followed by a diagnostic line. Doing so, each sub-component is fully tested (the first DTL tanks is the most difficult one), as well as the transitions which are crucial in a high-intensity/high-power accelerator (space charge regime).

Other development

The project is a 2×5 MW beam power project. This is one of the most powerful projects in the world (with ILC-International Linear Collider). Therefore it was always based on conservative specifications.

As the project is delayed, it might be interesting to support new developments like design based on superconducting cavities. This supposes that the new options MUST be compared at the same level than the reference design, to be able to prove their advantages.

The technical baseline will be frozen with the construction decision phase.

Other

During the year 2004, reviews were made on the present design, next R&D, schedule and costing with the Ad-Hoc committee and some of the accelerator team members.

One of the point explained by the Ad-Hoc Committee in the "technical assessment report" is that "In an aggressive realisation scenario it should be possible to shorten significantly the total time planned for the EVEDA, construction and commissioning phases (currently 15 years to full exploitation), which would be in the best interest of the Project's mission.". It is necessary to keep in mind that the EVEDA phase was proposed to allow a spreading of the investment over the years. It was also pointed out at the time of the suggestion that it could lead to a global cost increase.

CONCLUSIONS

We have a reference design. This design has to enter in a detailed study phase, with prototypes or final parts. Integration, RF system, engineering models have to be made. This supposes a major investment and a decision on ITER/IFMIF has to be pronounced. Such an "announce effect" might be crucial for the project.

The team needs to be reinforced, once the construction decision is made. The CEA-Saclay team is on a "waiting position". Even if the CEA-Saclay team is not directly involved in the near future development, they can answer questions that may arise on the linac design. The main contact persons are:

Pascal DEBU: pdebu@cea.fr	Head of the SACM laboratory
Pierre-Yves BEAUVAIS: pybeauvais@cea.fr	IPHI project leader
Pierre-Emmanuel BERNAUDIN: pebernaudin@cea.fr	DTL hot model
Aline CURTONI: acurtoni@cea.fr	2D RFQ optimization
Michel DESMONS: mdesmons@cea.fr	RF
Romuald DUPERRIER: rduperrier@cea.fr	Beam dynamics – end-to-end
Robin FERDINAND: robin.ferdinand@cea.fr	former task leader
Alain FRANCE: afrance@cea.fr	RFQ tuning
Raphael GOBIN: rjgobin@cea.fr	ECR source
Jacques PAYET: jpayet@cea.fr	HEBT
Didier URIOT: duriot@cea.fr	Beam dynamics – end-to-end

REFERENCES

[1] P-Y. Beauvais - Status report on the construction of the French high intensity proton injector (IPHI) - proceeding of EPAC 2002, Paris, page 539-541.

[2] R. Gobin et al. - High intensity ECR ion source (H+, D+, H-) developments at CEA Saclay - ISIS2001 conference, RSI, Vol.73, n°2, February 2002 (922).

[3] SPIRAL 2 white book - To be published in May.

[4] SNS Beam commissioning status - S. Henderson et al. - Proc. EPAC 2004, p. 1524.

[5] Beam Dynamics and Commissioning of the J-PARC Linac - Y. Yamazaki et al. - Proc. EPAC 2004, p. 1351.

[6] The GSI synchrotron facility proposal for acceleration of high intensity ion and proton beams - P. Spiller et al. Proc. PAC 2003, p. 589.

TASK LEADER

Robin FERDINAND

DSM/DAPNIA/SACM
CEA-Saclay
F-91191 Gif-sur-Yvette Cedex

Tél. : 33 1 69 08 96 91
Fax : 33 1 69 08 14 30

E-mail : robin.ferdinand@cea.fr